Analytical investigation of the minimization of the total radiated sound power from a vibrating plate

Mehran Hajilou[1], Delf Sachau[2]

[1] Helmut Schmidt University, 22043 Hamburg, E-Mail: hajiloum@hsu-hh.de
[2] Helmut Schmidt University, 22043 Hamburg, E-Mail: sachau@hsu-hh.de

Abstract

Active-Noise-Control (ANC) is a method for reducing unwanted so-called primary sound by destructive interference with sound generated by so-called secondary sources (loudspeakers). The latter are specifically designed to cancel the primary noise. The design requirements of ANC-systems are related to the theory of reducing the sound power of a primary source by monopole secondary sources.

In this paper the primary source is a vibrating simply supported plate which is radiating sound into free field. The loudspeakers are placed in front of the plate. The optimal volume velocities for the sound reduction are calculated by minimizing the radiated sound intensity in front of each monopole source in order to minimize the total radiated sound power of the primary and secondary sources. The analytical calculations are carried out with one and two loudspeakers. The optimal position of the secondary sources in front of the plate is studied in consideration of a high sound reduction.

Total Active Sound Power Minimization (TASPM)

Figure (1) shows the system of sound minimization which includes the primary and secondary sources and also a controller. In this investigation, the primary source is a simply supported plate in an infinite baffle which is excited by a point force, and the secondary sources are the loudspeakers in front of the plate.

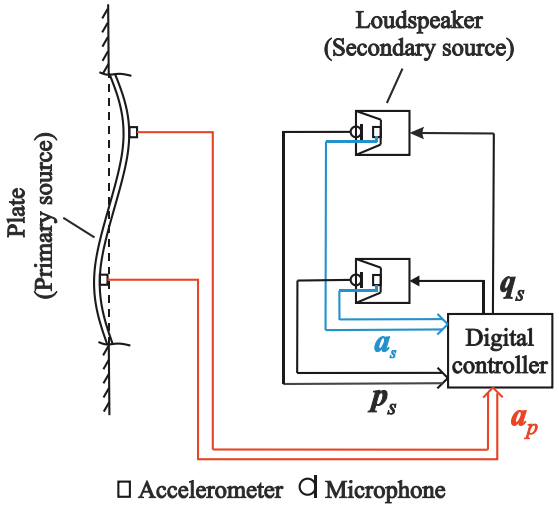

Figure 1: Schematic of a MIMO system in TASPM [3]

As shown in Figure (1), the input data in the MIMO (Multiple Input Multiple Output) system are the measurements of the normal surface accelerations of the primary source $\boldsymbol{a}_p = [a_{p1} \quad a_{p2}]^T$, acceleration of the secondary sources $\boldsymbol{a}_s = [a_{s1} \quad a_{s2}]^T$ and also the sound pressures in front of the secondary sources $\boldsymbol{p}_s = [p_{s1} \quad p_{s2}]^T$.

In order to minimize the total radiated sound power of the primary and secondary sources, TASPM has been suggested by Böhme [1] as a new approach in the field of ANC. This approach involves minimizing sound intensity in front of each secondary source which enables the total radiated sound power of the primary and secondary sources to be reduced. In other words:

$$\boldsymbol{I}_s = \begin{bmatrix} I_{s1} \\ I_{s2} \end{bmatrix} = \begin{bmatrix} 0 \\ 0 \end{bmatrix} \tag{1}$$

wherein I_{sl} with $l = 1,2$ are the active sound intensities I_l of each secondary source. The radiated sound intensities of the secondary sources can be extended as below:

$$\boldsymbol{I}_s = -\frac{1}{2\omega}\,\mathrm{Im}\{\mathrm{diag}\{\boldsymbol{p}_s(j\omega)\}\boldsymbol{a}_s^*(j\omega)\} \tag{2}$$

where diag{ . } is the diagonal matrix of the quantity in brackets, $*$ denotes complex conjugation, Im{.} is the imaginary part and ω is the angular frequency. The term $j\omega$ for each parameter in Equation (2) means that each parameter is a complex number at each angular frequency ω.

TASPM introduces an optimal factor $\mathcal{K}_l$ assigned to each secondary source. With real amplification factors defined to be $\boldsymbol{\mathcal{K}} = [\mathcal{K}_1 \quad \mathcal{K}_2]^T$, the secondary accelerations become:

$$\boldsymbol{a}_s(j\omega) = \mathrm{diag}\{\boldsymbol{\mathcal{K}}\}\,\boldsymbol{a}_p(j\omega) \tag{3}$$

The primary pressures $\boldsymbol{p}_{ps}(j\omega)$ are superimposed by the secondary pressures $\boldsymbol{p}_{ss}(j\omega)$ measured at the position of the microphones:

$$\boldsymbol{p}_s(j\omega) = \boldsymbol{p}_{ps}(j\omega) + \boldsymbol{p}_{ss}(j\omega) \tag{4}$$

The secondary pressures $\boldsymbol{p}_{ss}(j\omega)$

$$\boldsymbol{p}_{ss}(j\omega) = \boldsymbol{H}_{pa}(j\omega)\,\boldsymbol{a}_s(j\omega) \tag{5}$$

can be expressed by the transfer matrix $\boldsymbol{H}_{pa}(j\omega)$ between pressure in front and acceleration of each secondary source $\boldsymbol{a}_s(j\omega)$.

Substituting Equation (5) with Equation (4) in Equation (2) leads to:

$$\boldsymbol{I}_s = -\frac{1}{2\omega}\mathrm{Im}\{\,\mathrm{diag}\,\{\boldsymbol{p}_{ps}(j\omega) + \boldsymbol{H}_{pa}(j\omega)\,\mathrm{diag}\,\{\boldsymbol{a}_p(j\omega)\}\boldsymbol{\mathcal{K}}\}\,\mathrm{diag}\,\{\boldsymbol{a}_p^*(j\omega)\}\boldsymbol{\mathcal{K}}\} \tag{6}$$

Hence, an optimal factor (control signal) for each secondary source $\boldsymbol{\mathcal{K}} = [\mathcal{K}_1 \quad \mathcal{K}_2]^T$ can be defined [1], [2]:

$$\boldsymbol{I}_s = 0 \rightarrow$$

$$\boldsymbol{\mathcal{K}} = -\mathrm{Im}\{\,\mathrm{diag}\,\{\boldsymbol{a}_p^*(j\omega)\}\boldsymbol{H}_{pa}(j\omega)\mathrm{diag}\,\{\boldsymbol{a}_p(j\omega)\}\}^{-1}$$

$$\mathrm{Im}\{\mathrm{diag}\{\boldsymbol{p}_{ps}(j\omega)\}\boldsymbol{a}_p^*(j\omega)\} \tag{7}$$

Finally, the formulated optimal volume velocities $\boldsymbol{q}_s = [q_1 \quad q_2]^T$ of the secondary sources can be introduced:

$$\boldsymbol{q}_s(j\omega) = S_s\,\boldsymbol{v}_s(j\omega) \tag{8}$$

where $\boldsymbol{v}_s$ are the velocity of the membrane secondary sources. S_s is the area of the membrane of the secondary source with the radius R_s. Equation (8) can be rewritten in terms of acceleration $a_s(j\omega)$ with $a_s(j\omega) = j\omega v_s(j\omega)$:

$$\boldsymbol{q}_s(j\omega) = \frac{S_s}{j\omega}\, \boldsymbol{a}_s(j\omega) \tag{9}$$

Substituting Equation (3) in Equation (9) leads to:

$$\boldsymbol{q}_s(j\omega) = -\frac{S_s\, j}{\omega}\big(\mathrm{diag}\{\boldsymbol{\mathcal{K}}\}\, \boldsymbol{a}_p(j\omega)\big) \tag{10}$$

The numerical calculation of $\boldsymbol{\mathcal{K}}$ from Equation (7) requires the analytical calculation of the acoustic primary pressures $\boldsymbol{p}_{ps}(j\omega)$ and transfer matrix of secondary sources $\boldsymbol{H}_{pa}(j\omega)$.

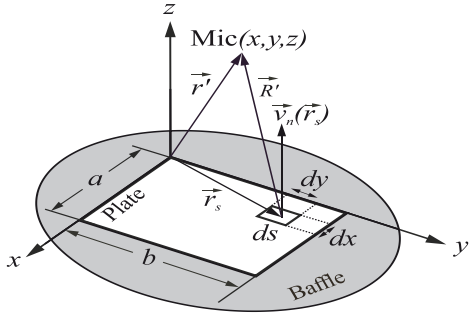

Figure 2: Microphone in front of a rectangular plate in Cartesian coordinate

Figure (2) represents the surface of a rectangular plate with dimensions (a, b) located in xy-plane in a coplanar rigid baffle. $\vec{r'}$ is the position vector of the observation point $\mathrm{Mic}(x, y, z)$. Furthermore, $\vec{r_s}$ is the position vector of the surface element ds having normal velocity amplitude $v_n(\vec{r_s})$ and R'=$|\vec{r'} - \vec{r_s}|$. The surface element $\mathrm{d}s = dx\, dy$.

The primary pressure p_{ps} at the position of the microphone in free field can be formulated by Rayleigh′s first integral [4]:

$$p_{ps}(\vec{r'}, \omega) = \frac{j\,\omega\,\rho_0}{2\,\pi} \int_S v_n(\vec{r_s})\, \frac{e^{-jkR'}}{R'}\, ds \tag{11}$$

where S denotes the surface area of the plate, the wavenumber $k = \omega/c_0$, wherein c_0 is the speed of the sound and ρ_0 is the density of the air.

The Rayleigh integral can be written in discrete form. To get this, the surface of the plate is divided into N rectangular elements Δs of equal size, which are small compared to the acoustic wavelength. It is assumed that the normal velocity is constant across each element. So, the primary pressure p_{ps} is the sum of the sound pressure of each elemental source at the observation point $\mathrm{Mic}(x, y, z)$:

$$p_{ps}\left(\vec{r'}, \omega\right) = \frac{j\,\omega\,\rho_0}{2\,\pi} \sum_{n=1}^{N} v_n(\vec{r_s})\, \frac{e^{-jkR'}}{R'}\, \Delta s \tag{12}$$

Furthermore, the formulation of $\boldsymbol{H}_{pa}(j\omega)$ can be done by rewriting Equation (5) in terms of velocity $v_s(j\omega)$ with $v_s(j\omega) = \frac{1}{j\omega} a_s(j\omega)$:

$$\boldsymbol{H}_{pa}(j\omega) = \frac{1}{j\omega}\, \boldsymbol{p}_{ss}(j\omega)\, \boldsymbol{v}_s{}^{-1}(j\omega) \tag{13}$$

Equation (13) can be reformulated in terms of the secondary volume velocities $\boldsymbol{q}_s(j\omega)$ by substituting Equation (8) in Equation (13):

$$\boldsymbol{H}_{pa} = \frac{S_s}{j\omega} \boldsymbol{p}_{ss}(j\omega)\, \boldsymbol{q}_s{}^{-1}(j\omega) \tag{14}$$

$\boldsymbol{Z}$ relates the complex acoustic pressures $\boldsymbol{p_{ss}}$ at the position of each secondary source to the strength of each secondary source $\boldsymbol{q}_s$ [5]. By substituting $\boldsymbol{Z}$ [5] in Equation (14), $\boldsymbol{H}_{pa}$ can be rewritten as:

$$\boldsymbol{H}_{pa} = -\frac{j\, S_s \omega\, \rho_0}{2\,\pi\, c_0} \tag{15}$$

$$\begin{bmatrix} 1 & \dfrac{\sin(k\, R_{12})}{kR_{12}} + j\dfrac{\cos(k\, R_{12})}{kR_{12}} \\ \dfrac{\sin(k\, R_{12})}{k\, R_{12}} + j\dfrac{\cos(k\, R_{12})}{kR_{12}} & 1 \end{bmatrix}$$

where R_{12} is the distance between the first and second secondary sources.

Global sound reduction using TASPM

The theory of total radiated sound from the primary and secondary sources in the far field is suggested by Deffayet [5]. Figure (3) shows a plate which is surrounded by a hemisphere in the far field. The center of the hemisphere is at one corner of the plate. The observation point $P_f(r, \theta, \varphi)$ is on the surface of the hemisphere.

Furthermore, two loudspeakers at distance d from the plate are considered.

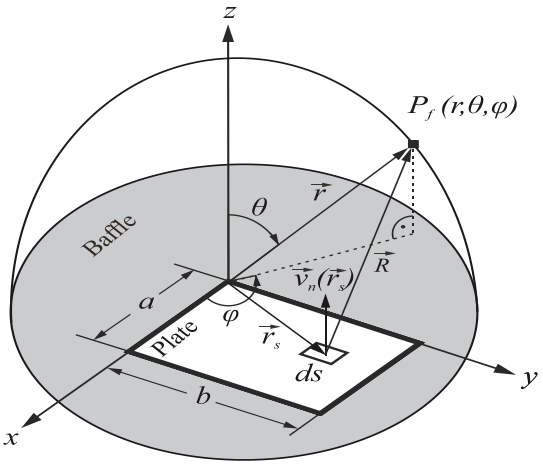

Figure 3: Rectangular plate with observation point $P_f(r, \theta, \varphi)$ in the far field

Total radiated sound power Π_t in the far field formulated by the combination of the sound power of the primary source Π_p and secondary sources Π_s is given by:

$$\Pi_t = \Pi_p + \Pi_s + \sum_{l=1}^{2} \Pi_l \tag{16}$$

Π_l is the radiated sound power produced by the interference of the primary pressure $p_p(\vec{r}, \omega)$ and the l-th secondary pressure $p_l(\vec{r_l}, \omega)$ in the far field:

$$\Pi_l = \int_0^{2\pi} \int_0^{\frac{\pi}{2}} \frac{p_p(\vec{r}, \omega)\, p_l{}^*(\vec{r_l}, \omega) + p_p{}^*(\vec{r}, \omega)\, p_l(\vec{r_l}, \omega)}{2\,\rho_0\, c_0} \tag{17}$$

$$|\vec{r}|^2 \sin\theta\; d\theta\; d\Phi$$

The pressure radiated by the l-th loudspeaker in far field is:

$$p_l(\vec{r_l}, \omega) = \frac{j\,\omega\,\rho_0}{2\,\pi} q_l(\omega) e^{-jk\,|\vec{r} - \vec{r_l}|} \tag{18}$$

where q_l is the l-th complex secondary source strength and $|\vec{r} - \vec{r_l}|$ is the distance between the l-th loudspeaker and point of observation in the far field.

The total sound power output from the array of the secondary sources Π_s can be written as:

$$\Pi_s = \boldsymbol{q}_s^H \boldsymbol{A}\, \boldsymbol{q}_s \tag{19}$$

where H denotes the conjugate of the transpose vector, $\boldsymbol{A} = \frac{1}{2}\,\mathrm{Re}\{\boldsymbol{Z}\}$ and Re{.} is the real part. ′

Results

To get the effectiveness of the TASPM, the numerical calculations are carried out by substituting the optimal secondary volume velocity formulated by the TASPM, namely Equation (8), in Equation (16). In Table (1), the parameters listed are used in the numerical calculation

Table 1: Parameters of the model designed in Figure (3)

Parameter	Variable	Value
Dimension of plate	(a, b)	(35,45) cm
Thickness of plate	h	2 mm
Coordinate of excitation point (EP)	(x_g, y_g)	(28.5,38.5) cm
Amplitude of the point force	F	2 N
Damping loss factor of plate	ξ	0.01
Density of aluminum plate	ρ	2700 kg/m^3
Poisson's ratio of plate	ν	0.33
Young's modulus of plate	E	70 × 10^9 Pa
Speed of sound	c_0	343 m/s
Density of air	ρ_0	1.2041 kg/m^3
Radius of hemisphere	r	100 cm
Radius of loudspeaker's membrane	R_s	7 cm
Distance between plate and loudspeaker	d	20 cm

The number and positions of the secondary sources in front of the plate are determined by the class of the radiated mode of the vibrating plate. Therefore, a mode analysis [4] is carried out for a free vibrating simply supported plate in order to define the number of modes (m, n) involved on the surface of the plate associated with eigenfrequencies:

$$\omega_{mn} = \sqrt{\frac{D}{\rho h}\left[\left(\frac{m\pi}{a}\right)^2 + \left(\frac{n\pi}{b}\right)^2\right]} \tag{20}$$

where ω_{mn} is the eigenfrequency of the plate, (m, n) are integers of the vibrating mode of the plate in the x, y directions respectively, ρ is the density of the plate and the stiffness of the plate $D = \frac{E\,h^3}{12(1-\nu^2)}$.

Figure (5) presents the numerical results. The red line belongs to the radiated Sound Power Level (SPL) of the primary source in the absence of any secondary sources. The results are calculated in the frequency domain which ranges from 55 to 300 Hz with step frequency $f_{step} = 5$ Hz.

The peaks on the red line in Figure (5) happen at eigenfrequencies 64 Hz, 136 Hz, 183 Hz, 256 Hz of the plate. The complex primary displacement generated at the position $x_p(x, y)$ by a point force at position (x_g, y_g) is given by [4]:

$$x_p(x, y, \omega) = \frac{F(\omega)}{\rho h a b}\sum_{m=1}^{5}\sum_{n=1}^{5}\frac{Q_{mn}(x, y)\, Q_{mn}(x_g, y_g)}{[\omega_{mn}^2(1 + j\,\xi) - \omega^2]} \tag{21}$$

in which the mode shape of a simply supported rectangular plate is [4]:

$$Q_{mn}(x, y) = 2\sin\left(\frac{m\pi x}{a}\right)\sin\left(\frac{n\pi y}{b}\right) \tag{22}$$

x_p in Equation (21) can be rewritten in terms of acceleration a_p with $a_p = -\omega^2 x_p$. In the numerical calculation, the first 25 modes of the plate are considered.

Results with one loudspeaker (Configuration I)

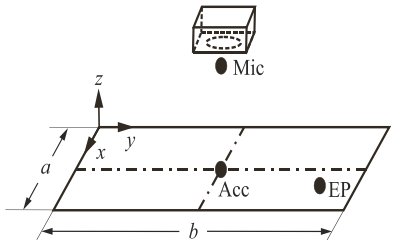

Figure 4: Schematic of the configuration I

Table 2: Position of the components in configuration I

Component	Coordinate		
	x	y	z
Loudspeaker	$\frac{a}{2}$	$\frac{b}{2}$	20 cm
Microphone (Mic)			18 cm
Primary accelerometer (Acc)			0 cm

Table (2) lists the position of each component in the configuration I. The position of each component is depicted in Figure (4) schematically. In this case, only one loudspeaker is placed in front of the plate.

The blue line in Figure (5) presents the results of the total SPL by TASPM in the configuration I.

Comparing the red and blue lines in Figure (5) reveals that the total radiated sound is minimized in the low frequencies up to $f \cong 125$ Hz. At the frequencies range from 125 Hz to 210 Hz, TASPM is not capable of minimizing the sound. The highest SPL reduction ($\cong$ 20 dB) occurs at $f \cong 64$ Hz. At this eigenfrequency and according to Equation (20), the plate has one antinode in the x, y directions, namely $(m, n) = (1,1)$.

The next eigenfrequency of the plate occurs at $f \cong$ 136 Hz where the plate has two antinodes in y direction, namely $(m, n) = (1,2)$. Comparing the red and blue lines at $f \cong 136$ Hz in Figure (5) shows that one loudspeaker is incapable of controlling the sound radiation from (1,2) mode.

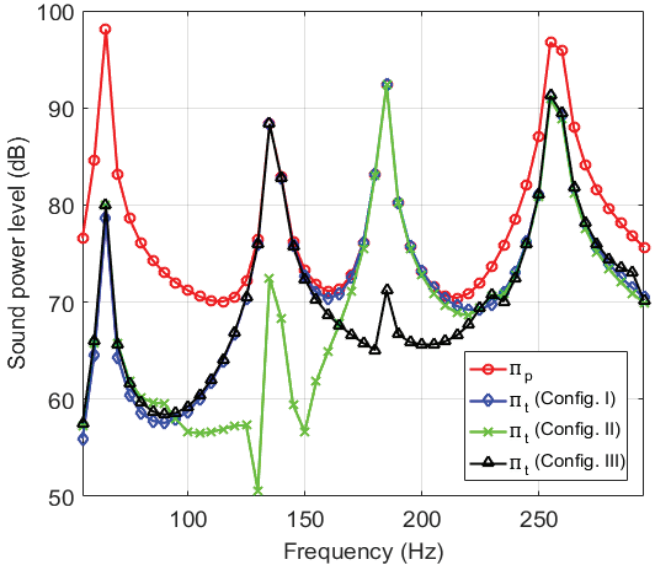

Figure 5: Results of the sound reduction by TASPM

Results with two loudspeakers (Configuration II)

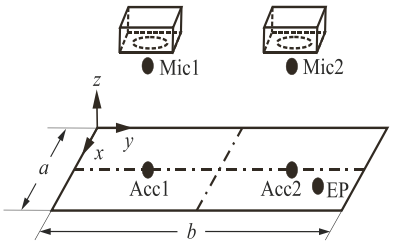

Figure 6: Schematic of the configuration II

Table 3: Position of the components in configuration II

Component		Coordinate		
		x	y	z
1st	Loudspeaker	$\frac{a}{2}$	$\frac{b}{4}$	20 cm
	Microphone (Mic1)			18 cm
	Primary accelerometer (Acc1)			0 cm
2nd	Loudspeaker		$\frac{3b}{4}$	20 cm
	Microphone (Mic2)			18 cm
	Primary accelerometer (Acc2)			0 cm

In this configuration, two loudspeakers are positioned in front of the antinodes of the plate at $f \cong 136$ Hz when $(m,n) = (1,2)$. The coordinate of position of each component is given in Table (3). Figure (6) presents the schematic of the components in the configuration II.

The green line in Figure (5) presents the results of total SPL in this trial. Comparing the red and green lines shows that the highest SPL reduction is about 17 dB at $f \cong 136$ Hz. Hence, positioning each loudspeaker in front of each antinode of the plate is the optimal position of each loudspeaker.

Furthermore, Figure (5) shows that the SPL minimization at $f \cong 64$ Hz in the configuration I and the configuration II is about 19 dB. Hence, achieving the highest sound reduction by TASPM requires to select the optimal number of the loudspeakers in front of the plate.

Moreover, Figure (5) shows no sound reduction at the higher frequencies such as $f \cong 183$ Hz where the next peak on the red line occurs.

Results with two loudspeakers (Configuration III)

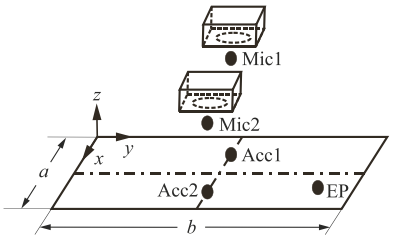

Figure 7: Schematic of the configuration III

Table 4: Position of the components in configuration III

Component		Coordinate		
		x	y	z
1st	Loudspeaker	$\frac{a}{4}$	$\frac{b}{2}$	20 cm
	Microphone (Mic1)			18 cm
	Primary accelerometer (Acc1)			0 cm
2nd	Loudspeaker	$\frac{3a}{4}$		20 cm
	Microphone (Mic2)			18 cm
	Primary accelerometer (Acc2)			0 cm

According to Equation (20), the next eigenfrequency of the plate happens at $f \cong 183$ Hz when $(m,n) = (2,1)$. At this frequency, the plate has two antinodes in the x direction.

To study the possibility of the sound reduction in the configuration III, the loudspeakers are placed in front of antinodes at $f \cong 183$ Hz. The coordinates of the positions of the loudspeakers are recorded in Table (4). The schematic of the components is presented in Figure (7).

The black line in Figure (5) presents the results in this trial. As one would expected, TASPM is capable of minimizing the total radiated sound at $f \cong 183$ Hz which is about 20 dB. Furthermore, the sound cannot be reduced at $f \cong 136$ Hz due to the inappropriate positions of the loudspeakers in front of the plate. At lower frequencies such as $f \cong 64$ Hz, the sound reduction is almost the same in comparison with the achieved results in the configuration I and configuration II.

Conclusion

The proposed TASPM method is feasible in order to give the best possible noise reduction for the given secondary source positions in front of the plate.

The number of loudspeakers necessary to reduce the total radiated sound power is related to the class of the radiating structural modes of the plate. For the (1,1) mode, one loudspeaker is sufficient to minimize the total radiated sound power. For the (1,2) or (2,1) mode, at least two loudspeakers are required to minimize the total radiated sound power.

The positions of the secondary sources in front of the vibrating plate have the significant effect on the total sound reduction by TASPM. The optimal positions of the loudspeakers are generally in front of the antinodes of the plate where the highest displacements occur.

Literature

[1] S. Böhme and D. Sachau, Practical implementation of a system for adaptive power minimization. In 18th International Congress on Sound and Vibration, 2011

[2] S. Böhme and D. Sachau, Single channel system for adaptive power minimization. In: Internoise. 39th International Congress on Noise Control Engineering

[3] U. Krause and D. Sachau, Active noise control experiment minimizing radiation of active energy. In: De Clerck (Hg.): Conference Proceedings of the Society for Experimental Mechanics Series, Bd. 8. Experimental Techniques, Rotating Machinery and Acoustics. The Society for Experimental Mechanics, 2015

[4] F. Fahy and P. Gardonio, Sound and structural vibration. Second edition 2007, Chapter 2, 3

[5] C. Deffayet and P. A. Nelson, Active control of low-frequency harmonic sound radiation by a finite panel. Journal of the Acoustical society of America, 1988